Nighttime *D* region electron density profiles and variabilities inferred from broadband measurements using VLF radio emissions from lightning

Zhenggang Cheng,[1] Steven A. Cummer,[1] Daniel N. Baker,[2] and Shrikanth G. Kanekal[3]

Received 7 July 2005; revised 16 January 2006; accepted 19 January 2006; published 5 May 2006.

[1] Lightning discharges radiate most of their electromagnetic energy in the very low frequency (VLF, 3–30 kHz) and extremely low frequency (ELF, 3–3000 Hz) bands and are, consequently, an effective tool for remotely sensing the nighttime ionospheric *D* region electron density profile. Using broadband lightning-generated VLF signals, we derived the night-to-night variations of the midlatitude ionospheric *D* region electron density profiles. For 16 nights, between 1 July and 4 August 2004, we examined measured VLF data from lightning occurring near the United States east coast (~530–860 km away from Duke University) and received at Duke University from 0400 to 0600 UT. From these observed VLF radio atmospherics (sferics), we extracted the nighttime *D* region electron density profiles covering the range of electron densities from 10^0 to 10^3 cm^{-3}, in the altitude range of approximately 70–95 km, using a two-dimensional, laterally homogenous model of VLF propagation in the Earth-ionosphere waveguide. The inferred electron density profile variabilities were in good agreement with those from past nighttime rocket experiments at similar latitudes. Using the rocket-measured profiles in our propagation simulations, we determined that the two-parameter exponential *D* region electron density profiles we inferred were the best exponential fit, in the electron density range of ~3 to ~500 cm^{-3}, to the rocket-measured *D* region electron density profiles. In an initial effort to determine the sources of the observed variabilities, we compared the SAMPEX precipitating electron measurements to the electron density profiles inferred during July 2000. The results indicate that high-energy electron precipitation might account for at least part of the night-to-night variations of the *D* region electron densities at the midlatitudes.

Citation: Cheng, Z., S. A. Cummer, D. N. Baker, and S. G. Kanekal (2006), Nighttime *D* region electron density profiles and variabilities inferred from broadband measurements using VLF radio emissions from lightning, *J. Geophys. Res.*, *111*, A05302, doi:10.1029/2005JA011308.

1. Introduction

[2] Because it is relatively inaccessible, the ionospheric *D* region (<95 km) is one of the least studied regions of Earth's atmosphere. The altitudes (~70–95 km) of this region are far too high for balloons and too low for most satellites to reach, making continuous monitoring of the ionospheric *D* region difficult. To obtain electron density profiles by rockets, various probing techniques [*Holt and Lerfald*, 1967; *Smith*, 1969; *Danilov and Vanina*, 2001], the exploitation of ionospheric radio wave propagation (differential absorption, Faraday rotation [*Jacobsen and Friedrich*, 1979; *Friedrich and Torkar*, 2001; *Mechtly et al.*, 1967], and the coherent frequency technique [*Seddon*, 1953]) have been applied. Although these in situ measurements are precise, the rocket techniques can be used only episodically and at a limited number of locales. Ground-based measurements make it possible to monitor the state of the *D* region ionosphere more routinely. These techniques include the cross modulation [*Fejer*, 1970], partial reflection [*Newman and Ferraro*, 1976], and incoherent scatter [*Mathews et al.*, 1982] methods; however, the incoherent scatter technique is difficult to apply when the nighttime *D* region electron density is less than 10^3 cm^{-3} [*Hargreaves*, 1992, p. 81].

[3] Because VLF waves are nearly completely reflected by the *D* region, signals from a single frequency VLF transmitter are a useful tool for measuring electron density in this altitude range. Steep and oblique incidence VLF and LF radio wave reflection data have been inverted to derive *D* region electron density profiles [*Deeks*, 1966; *Thomas and Harrison*, 1970]. Single-frequency VLF propagation measurements have been used to estimate the *D* region electron density parameters along a given propagation path [*Bickel et al.*, 1970; *Thomson*, 1993]. Phase-coherent,

[1]Department of Electrical and Computer Engineering, Duke University, Durham, North Carolina, USA.
[2]Laboratory for Atmospheric and Space Physics, University of Colorado, Boulder, Colorado, USA.
[3]Space Environment Center, NOAA, Boulder, Colorado, USA.

0148-0227/06/2005JA011308$09.00

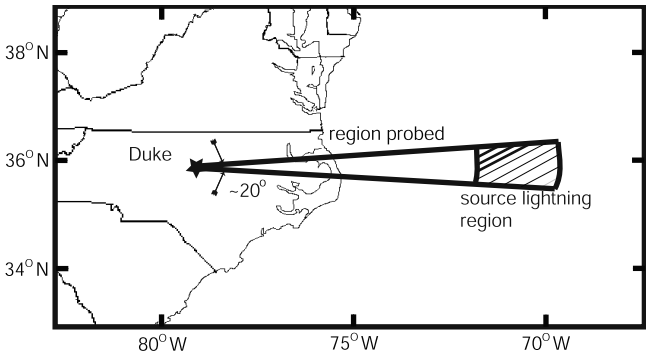

Figure 1. Map showing the location of the source lightning and the probed region.

narrowband VLF data recorded at multiple sites have also been used to determine nighttime lower ionospheric electron density profiles [*Bainbridge and Inan*, 2003].

[4] *Cummer et al.* [1998] developed a different nighttime *D* region measurement technique based on wideband, long-distance VLF propagation effects observed in sferics, the electromagnetic signals launched by individual lightning discharges. This technique is significantly different from some of those mentioned above in that it is not a point measurement; rather, it is sensitive to the average electron density profile across the entire path and is therefore uniquely capable of measuring the electron density of large regions. As long as there are lightning strokes at target locations, we are able to monitor the state of the nighttime *D* region ionosphere over the propagation path between the lighting source and the receiver.

[5] In this work, we have applied this technique to derive the night-to-night variations of the *D* region ionosphere electron density over the east coast of the United States from 1 July to 4 August 2004, and we have compared the measurement results to the results of past nighttime rocket experiments which had been made at similar latitudes and found that our results are very consistent with those from rocket experiments. By using rocket-measured profiles in our propagation simulations, we determined that our inferred *D* region electron density profile is the best exponential fit, in the electron density range of $\sim$3 to $\sim$500 cm^{-3}, to the rocket-measured *D* region electron density profile. For the purpose of explaining the source of the night-to-night variations of the *D* region electron densities, we have presented our comparisons of the SAMPEX data with our measurement results of July 2000.

2. Sferic Observations

[6] We continuously recorded the broadband ELF/VLF ($\sim$50–25000 Hz) magnetic field waveforms from lightning at a 100 kHz sampling frequency, with a one-pole 13 kHz low-pass filter and an eight-pole 25 kHz antialiasing low-pass filter, at Duke University during July and August of 2004. We used data from the National Lightning Detection Network (NLDN) to determine the precise time (an accuracy of greater than 1 ms) and location (an accuracy of within a few kilometers) [*Cummins et al.*, 1998] of the source lightning discharges. This enables us to make calculations of the distance and bearing from the source to Duke which are necessary to accurately model the propagation effects. According to the NLDN data of July and August of 2004, there were 16 days on which there were many lightning strokes within the region, defined from 530–860 km range and from within ±10 degrees to geographic east of our sensor, during the local nighttime period of 0400–0600 UT. The map showing the probed region is given in Figure 1.

[7] The lightning-radiated power peaks in the ELF and VLF radio bands [*Uman*, 1987, p. 119]. Because the Earth-ionosphere waveguide is bounded by highly conductive ground and ionosphere, electromagnetic pulses from lightning can propagate long distances in waveguide modes quasi-TE (QTE), quasi-TM (QTM), and quasi-TEM (QTEM), analogous to the wave modes TE, TM, and TEM, in an ideal parallel-plate waveguide [e.g., *Inan and Inan*, 1999, p. 739]. Since the ionosphere and thus the waveguide is anisotropic, the azimuthal (B_φ) and radial (B_r) components of the horizontal magnetic field of received sferics are nonzero. However, B_φ is much larger than the B_r component at most frequencies, and thus, for the maximum SNR, we analyzed this component of the measured signals. In addition, the information we sought is most readily quantified in the spectral amplitude of B_φ [*Cummer et al.*, 1998], and it is from this quantity that the ionospheric measurement was extracted. Therefore the spectrum of B_φ has been used in this work for comparison with simulations.

[8] The SNR of the spectrum of one single observed sferic is usually high enough such that the fine structure is visible, but an improvement in the SNR can provide a more accurate *D* region electron density measurement. The SNR is improved by time domain averaging in which a number of individual sferics from a small geographic area were accurately time aligned and averaged to decrease the noise and isolate the signal of interest. To produce an average sferic spectrum, we averaged the sferics that were determined by the NLDN to have originated in a 0.2° latitude by 0.2° longitude region ($\sim$18 km by 22 km at latitudes of the continental United States). On each day, the sferics were taken within a different 30-min period during the overall time window of 0400–0600 UT, which was long enough to include a sufficient number of sferics for effective averaging but short enough so that the large-scale *D* region density was not likely to change significantly [*Cummer et al.*, 1998]. In order to prevent a small number of big sferics from dominating the averaged spectra, we normalized the sferics by dividing them by their peak currents measured by the NLDN. Normalizing the sferics did not affect the ionosphere measurements made in this work because the measurements do not depend on the absolute field amplitude.

[9] The SNR was also improved by using a late-time filter which low-pass filtered a portion of the sferic waveform, from $\sim$4 ms after the start of the sferic to the end, because only frequency components below $\sim$10 kHz remain after the first $\sim$4 ms; the long-delayed, near-cutoff components become strongly attenuated with increasing frequency [*Cummer et al.*, 1998]. In this work, to eliminate noise, without affecting the signal of interest, we used a zero phase shift filter with a −6 dB cutoff frequency of 10 kHz.

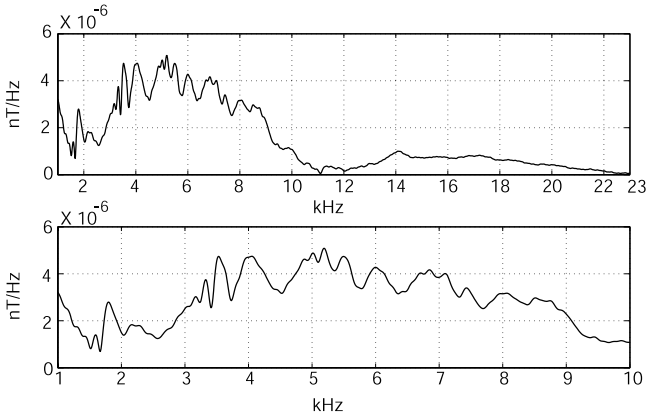

Figure 2. Average sferic spectrum from 10 sferics with later-time filtering and its fine structure.

[10] An example of the data produced by the averaging and late-time filtering procedures that have been described above is shown in Figure 2, with the top plot depicting the average sferic spectrum and the bottom plot emphasizing its fine structure. There were 10 sferics launched from the region 36.06° to 36.14°N and 72.01° to 72.19°W that met the criteria to be included in the averaging between 0414 and 0443 UT on 14 July 2004. A comparison of this spectrum with that of the individual sferic shows that the averaging and late-time filtering procedures improved the SNR and reinforced the fine spectral features that we have used as the basis of our VLF measurements. The inferred *D* region electron density profile is an average profile over the region of the propagation path between the lightning source and the receiver at Duke, for a 30-min period of VLF data averaging.

[11] The critical features in these spectra that enable the precise inference of *D* region parameters are the spectral variations between 3 and 10 kHz. These oscillations are produced by frequency-dependent interference between different propagating waveguide modes. As for all interferometric methods, the precise pattern of interference is very sensitive to small distance changes (in this case, the height of the ionosphere). These modal interference variations can be viewed as a fingerprint of the specific *D* region electron density profile. Although the lightning location accuracy of NLDN might be 1–2 km off the east coast of the United States [*Cummins et al.*, 1998], the error of location is very small compared to the sferic propagation distance that is approximately 600–900 km. Thus the influence of location error on our measurement is negligible.

3. Inferred Electron Density Profiles

[12] The *D* region ionosphere electron density profiles we infer are defined relative to the average ground altitude of the sferic propagation path. Thus the mean ground altitude of the sferic propagation path was added to the inferred ionosphere height parameter h' to consistently refer it to sea level. To infer the *D* region electron density profile, we compared the observed sferic spectrum with a model calculation [*Cummer et al.*, 1998]. The model calculation uses LWPC VLF-ELF propagation model [*Pappert and Ferguson*, 1986] that can account for finite ground conductivity, arbitrary background magnetic fields, and arbitrary electron density and collision frequency profiles. This model solves the time-harmonic propagation problem using the mode theory [*Budden*, 1961], in which the fields at a distance from the source have been described as a sum of independently propagating waveguide modes. The version of the LWPC model used in this study is a two-dimensional, laterally homogeneous model, assuming the same electron density profile along the entire propagation path.

[13] The electron density profile in the *D* region, the quantity we aimed to infer, is highly variable [*Budden*, 1985, p. 12]. We calculated the model sferic spectrum under a number of different ionospheres to find that which most closely matched the measured sferic spectrum. This procedure required a parameterization of the electron density profile so that it could be varied in a controlled manner. In this work, we have assumed that the *D* region electron density can be described by a two-parameter exponential profile,

$$N_e(h) = 1.43 \times 10^7 \exp(-0.15h') \cdot \exp\left[(\beta - 0.15)\left(h - h'\right)\right], \quad (1)$$

with h' in km and β in km^{-1} [*Wait and Spies*, 1964]. The two parameters, h' and β, control the height of the profile and the sharpness of the ionospheric transition, respectively. A larger β implies a more rapid change of N_e with altitude. This specific functional form has been used with success in previous comparisons between the VLF propagation theory and measurements [*Thomson*, 1993], and it has been found to agree with directly observed *D* region profiles [e.g., *Sechrist*, 1974].

[14] Through all of the reported simulations of the VLF propagation within the Earth-ionosphere waveguide, some of the waveguide parameters were assumed fixed. They are discussed below.

[15] 1. Ionospheric ion density: as a reasonable approximation to the known dominant ion species which are significant, but not dominant for propagation below 10 kHz, the LWPC propagation model simulates them as a single species with atomic mass 32 [*Narcisi and Bailey*, 1965]. As a rough approximation to the daytime observations of *Narcisi* [1971], we assumed that the positive ion density is constant below the altitude where N_e equals some predetermined value $N_i^{+\min}$ which is set equal to 3×10^2 cm^{-3}, a level at which the effect of ions is significant, but not overwhelming, and consistent with the observations of *Kopp et al.* [2003]. Thus $N_i^+ = N_i^{+\min}$ below this altitude and $N_i^+ = N_e$ above this altitude. To maintain charge neutrality, $N_i^- = N_i^+ - N_e$. The magnitude of the effect of a factor of 2 change in the ion density is small in terms of its effect on measured h' and β, and it did not significantly affect our ability to accurately infer the *D* region electron density profile [*Cummer et al.*, 1998].

[16] 2. Electron and ion collision frequency: the ionospheric electron-neutral collision frequency used in this work is an analytical approximation of experimental data and is given by *Wait and Spies* [1964] as

$$\nu_e = 1.816 \times 10^{11} \exp(-0.15h)\mathrm{s}^{-1}, \quad (2)$$

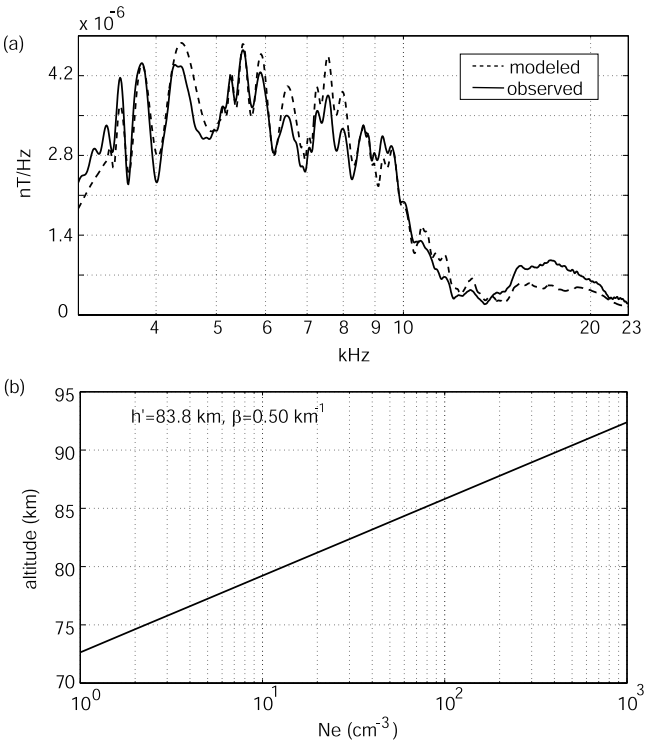

Figure 3. (a) Observed and best fit modeled sferic spectra on a frequency scale highlighting the fine structure agreement. (b) Measured *D* region electron density.

where h is the altitude measured in kilometers. The ion-neutral collision frequency is given by *Morfitt and Shellman* [1976] as

$$\nu_i = 4.54 \times 10^9 \exp(-0.15h)\mathrm{s}^{-1}, \quad (3)$$

for both positive and negative ions. Since ion and electron collision frequency profiles are less variable than the ion and electron density profiles [*Budden*, 1985, p.12], and, because modeling has shown that changing the collision frequencies by a factor of 2 has only a small effect on sferic propagation [*Cummer et al.*, 1998], we have assumed the electron and ion collision frequency profiles to be fixed.

[17] 3. Magnetic field parameters: the magnetic field parameters depended slightly on the precise path location but are given approximately by an amplitude of 5.0×10^4 nT, a dip angle of $\sim 70°$, and an azimuth (the angle of the wave propagation direction in degrees counterclockwise from geographic north) of $\sim 280°$ for the propagation paths studied, as shown in Figure 1.

[18] 4. Ground parameters: since more than one half to two third of the propagation path was covered by seawater, we set ground relative permittivity at 81 and ground conductivity at ~ 4 mho m^{-1}. It has been demonstrated that our measurement technique is relatively insensitive to the precise value of the assumed ground conductivity, provided it is greater than $\sim 3 \times 10^{-4}$ mho m^{-1} [*Cummer et al.*, 1998].

[19] 5. Lightning return stroke: the model return stroke has a current moment of [*Jones*, 1970]

$$I_m(t) = i_{g0}\frac{\nu_0}{\gamma}\left[e^{-at} - e^{-bt}\right]\left[1 - e^{-\gamma t}\right]. \quad (4)$$

Dennis and Pierce [1964], concluded from a review of data that reasonable parameter values are $i_{g0} = 20$ kA, $a = 2 \times 10^4$ s^{-1}, $b = 2 \times 10^5$ s^{-1}, $\nu_0 = 8 \times 10^7$ m s^{-1}, and $\gamma = 3 \times 10^4$ s^{-1}, and the values used to produce the spectra shown in this work are fixed, unless otherwise stated. Although changing the return stroke parameters a and b changes the general shape of the sferic amplitude spectrum, the modal interference variations that contain the information we used to extract the electron density profile do not depend on the source parameters. The measurement is thus not influenced by the return stroke parameters.

[20] For all sferics analyzed here, the precise lightning source location was known from NLDN data, and the propagation distance and the azimuth angle were fixed. Among all the Earth-ionosphere waveguide parameters, the ionosphere electron density profile has by far the strongest influence on the VLF sferic spectra. Thus we can infer the accurate electron density profile only by adjusting the electron density profile until the best agreement between the broad spectral amplitude of the modeled and observed spectra of sferics is achieved. The procedure by which we minimized the difference between the measured and modeled spectrum was based on the least squares method which is discussed by *Cummer et al.* [1998].

[21] We now present a *D* region measurement example. Ten sferics used originated in lightning from latitudes 35.69°–35.84°N and longitudes 71.65°–71.79°W on 11 July 2004, between 0417 and 0442 UT, and were all recorded at Duke University, 664 km away from the center of this source region. The average measured sferic spectrum for this case is shown in Figure 3a with the solid line, and the best fit modeled spectrum is shown in Figure 3a with the dashed line. Both are shown on a frequency scale that highlights the fine structure agreement.

[22] Figure 3b shows the electron density profile over the propagation path defined by the two parameters with $h' = 83.8$ km and $\beta = 0.50$ km^{-1} which we inferred from the best agreement between the average measured sferic spectrum and the modeled spectrum. Only the N_e range from 10^0 to 10^3 cm^{-3} is shown in Figure 3 because it is the N_e range to which the VLF propagation is most sensitive, as discussed by *Cummer et al.* [1998]. The precision of this measurement technique depends primarily on the signal SNR and the propagation distance. The longer the propagation distance of the sferic with better SNR, the more complicated and clearer the sferic spectrum characteristics of the modal interference variations, rendering the inferred h' and β more reliable. For all of the measurements shown here, a change in h' by 0.2 km or in β by 0.05 km^{-1} produced distinguishably worse agreement, demonstrating the degree of precision (error bars in Figure 4) of our measurements.

[23] The modeled spectrum in Figure 3a was calculated using a model lightning return stroke with parameter values $a = 2.5 \times 10^4$ s^{-1} and $b = 2.5 \times 10^5$ s^{-1} in the notation of (4). These parameters were chosen to give good visual agreement between the broad spectral amplitude of the

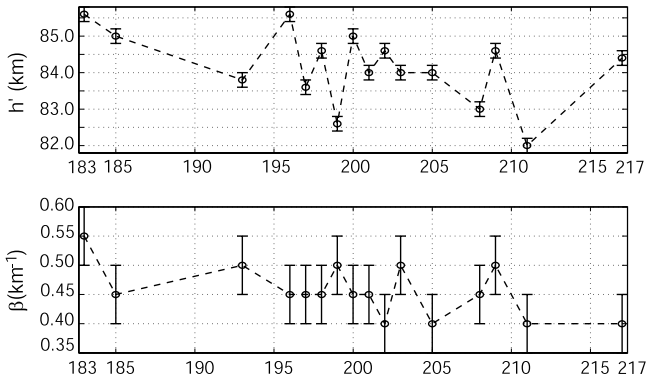

Figure 4. Variations of nighttime ionospheric *D* region height and sharpness parameters h' and β with days from 1 July to 4 August 2004.

modeled and observed spectra and to highlight the overall agreement between the modeled and observed spectra.

[24] Using the same technique, the nighttime electron density profiles of the probed region on the other 15 days were inferred with the maximum number of sferics for averaging equal to 20, minimum number equal to five and mean number equal to 12. The complete measurement results from 1 July to 4 August 2004, are summarized in Figure 4 and Figure 5 below.

[25] Figure 4 shows the variations of the nighttime ionospheric height parameter h' and sharpness parameter β on the days from 1 July to 4 August 2004, and Figure 5 shows the statistical distributions of the inferred h' and β during the same period. Figures 4 and 5 indicate that the nighttime ionospheric *D* region is far from static. The ionospheric height parameter h' during that period is bounded between 82.0 ± 0.2 and 85.6 ± 0.2 km. However, for 13 out of 16 days, the inferred h' is within the range of 83.6 ± 0.2 to 85.6 ± 0.2 km, with the mean value equal to 84.5 ± 0.2 km, and, for only three out of 16 days, h' is below 83.0 ± 0.2 km. The ionospheric sharpness parameter β during that period is bounded between 0.40 ± 0.05 and 0.55 ± 0.05 km^{-1}. However, for 15 out of 16 days, the inferred β is within the range of 0.40 ± 0.05 to 0.50 ± 0.05 km^{-1}, with the mean value equal to 0.45 ± 0.05 km^{-1}, and, for only one day, β is greater than 0.50 ± 0.05 km^{-1}.

4. Comparison With Rocket-Measured Profiles

[26] Because measuring *D* region electron density profiles is difficult, it is also difficult to compare our measurements to simultaneous measurements using other techniques. To confirm that our inferred profiles were reasonable in the context of past measurements, we compared our profiles with rocket-based profiles measured using the Faraday rotation technique. Of the 274 *D* region reliable electron density profiles collected by *Friedrich and Torkar* [2001], eight were measured at midlatitude sites near the United States east coast during the nighttime period from 0300 UT to 1000 UT. Among these eight profiles, only two (profiles b and d in Figure 6) were measured during the nighttime period from 0400 UT to 0600 UT, the same time period used in our measurements; only three (profiles a, b, and c in Figure 6) were measured in the summer during July and early August, the same time frame used in our measurements. Thus we chose these four (profiles a, b, c, and d in Figure 6) rocket-measured profiles and compared them to our inferred profiles in Figure 6.

[27] Profiles a, b, and c were measured in the summer (July/August) nighttime and profile d was measured in the winter (January) nighttime. The span of our inferred nighttime ionospheric *D* region electron density variations is in good agreement with the span of the rocket-measured nighttime ionospheric *D* region N_e profiles, although they were not time and space averaged on the same scales as our VLF-inferred *D* region N_e profiles. We conclude that our measurements are generally consistent with past direct measurements.

[28] Our two-parameter measurement technique smoothes out sharp variations that are at least sometimes present in the *D* region. To better understand the relationship between direct local and our indirect measurements, we used the rocket-measured profiles as input to our LWPC propagation model. We then used the output spectrum as an artificial, "measured" spectrum, and determined the exponential profile most consistent with this spectrum (as we do for measured data). Figure 7a shows the artificial measured

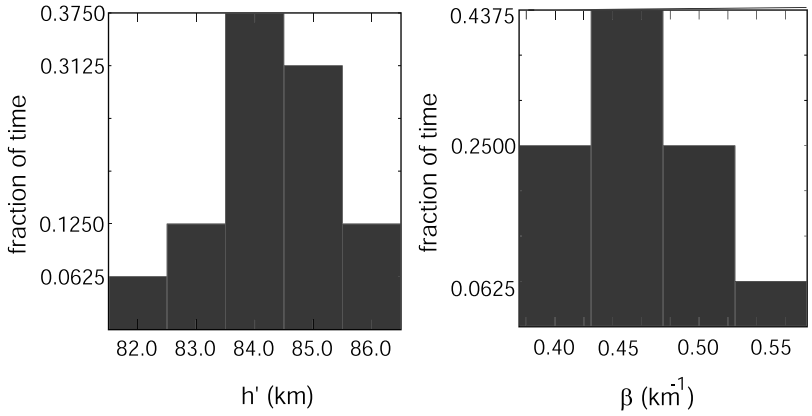

Figure 5. Statistical distributions of nighttime ionospheric *D* region height and sharpness parameters h' and β with days from 1 July to 4 August 2004.

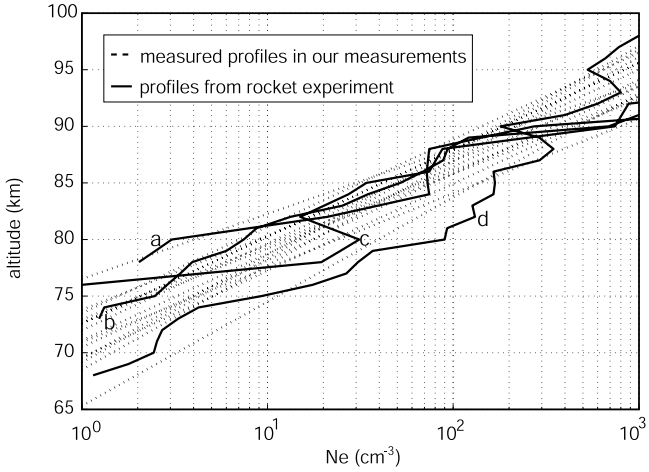

Figure 6. Comparison of the nighttime profiles derived from our measurements and those from nighttime rocket experiments: profiles a and c, 15 July 1964 [*Mechtly and Smith*, 1968]; profile b, 10 August 1977 [*Smith and Gilchrist*, 1984]; and profile d, 5 January 1978 [*Smith and Gilchrist*, 1984].

spectrum using the exact, rocket-measured profile (with a 664 km propagation distance) and the closest signal spectrum reproduced with a two-parameter exponential profile. They are in good agreement, confirming that an equivalent exponential profile reproduces the main propagation effects. The differences between these spectra are similar in magnitude to the differences between the experimentally measured and the two-parameter best fit spectra (see Figure 3). This observation suggests that the main source of the small disagreement between the measured and model spectra lies in the details of the electron density profile.

[29] In Figure 7b, profiles a′, b′, and c′ are the equivalent exponential N_e profiles of the rocket-measured N_e profiles a, b, and c, respectively. Through analysis of the three rocket-measured profiles, we determined that the best single exponential approximation of the rocket-measured profile was the exponential profile that resulted from a linear fit to log (N_e) over the electron density range from ~3 to ~500 cm^{-3}; the fit exponential profiles were very close to the measured equivalent exponential profiles of the original rocket-measured profiles, with the difference of h' within 0.6 km and the difference of β within 0.05 km^{-1}. This observation indicates that the electron densities ranging from ~3 to ~500 cm^{-3} plays the primary role in reflecting the VLF wave energy during the nighttime, and confirms that this technique measures an equivalent exponential profile which is essentially the best exponential fit, in the electron density range of ~3 to ~500 cm^{-3}, to the actual electron density profile.

5. Possible Sources of Variability

[30] Ionospheric *D* region electron density variability can be caused by external sources such as high-energy electron/proton precipitation [*Baker et al.*, 1993a], as well as solar flares [*Thomson et al.*, 2005], γ-ray flares [*Inan et al.*, 1999], and meteors [*Chilton*, 1961]. High-energy (>50 keV, although it depends somewhat on the ambient density of the atmosphere) electron precipitation can penetrate below 90 km, enhancing the *D* region electron density and, thereby, decreasing the ionospheric height parameter h', while lower-energy electrons do not penetrate to these altitudes [*Rees*, 1989]. *Kikuchi and Evans* [1983] found that the occurrence of ionospheric *D* region disturbances is well correlated with an increase in the precipitation of >300 keV electrons at high latitudes. *Cummer et al.* [1997] observed that precipitating energetic (>100 keV) particles account for the variations of the nighttime ionospheric *D* region electron densities in the auroral area.

[31] In order to investigate the source of the nighttime ionospheric *D* region electron density variations, we have examined the correlation between the energetic particle flux at the L shell of the propagation path and the corresponding nighttime ionospheric height parameter h' over that region. We compared high-energy (2–6 MeV) electron fluxes recorded by the Proton/Electron Telescope (PET) [*Cook et al.*, 1993] on board the Solar Anomalous and Magnetospheric Particle Explorer (SAMPEX) [*Baker et al.*, 1993b] with our *D* region electron density profile measurements from July 2000 to determine whether the variations in each measurement were correlated. We assumed that the SAMPEX measured particle precipitation fluxes at a given L shell averaged across the entire Earth over a day can be used to represent the fluxes at a specific location that is on that L shell.

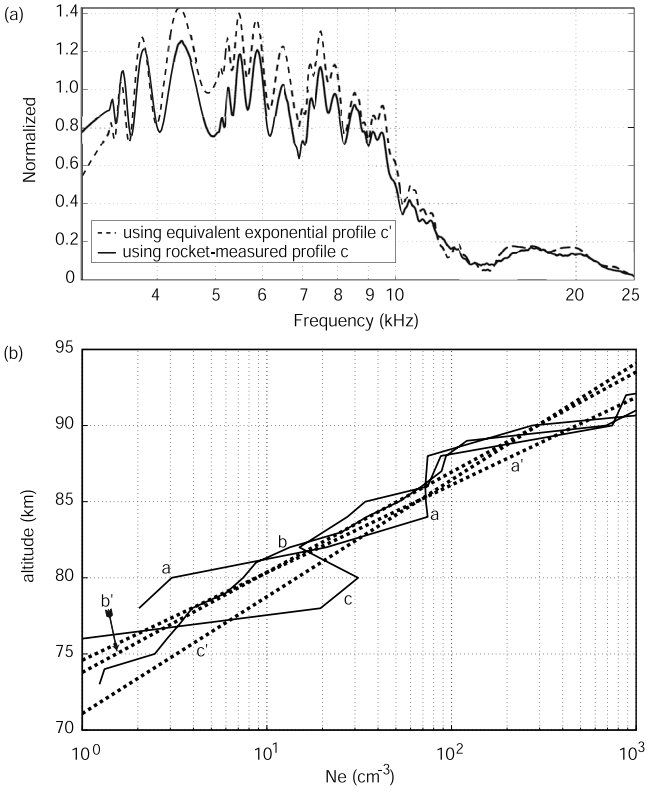

Figure 7. (a) Modeled sferic spectra using two different profiles c and c′. (b) Comparison of the rocket-measured nighttime profiles and their equivalent exponential profiles: profiles a and c, 15 July 1964 [*Mechtly and Smith*, 1968] and profile b, 10 August 1977 [*Smith and Gilchrist*, 1984].

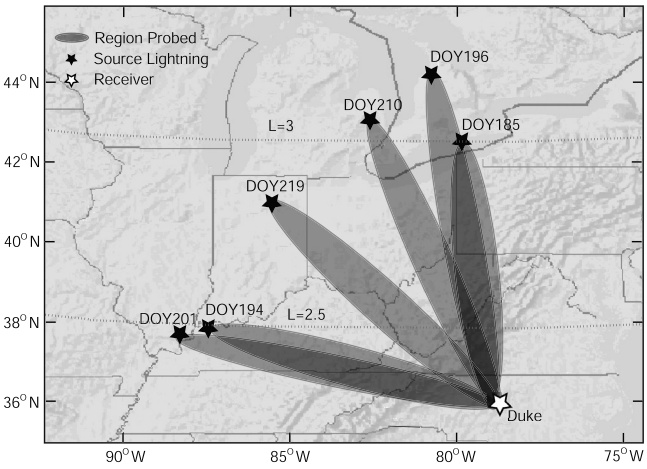

Figure 8. Measurement map for 6 nights in July 2000 from DOY 185 (3 July 2000) to DOY 210 (28 July 2000).

The main energy deposition altitude of 2–6 MeV electrons is between 40 and 55 km [*Brasseur and Solomon*, 1984, p. 326] which is below the primary VLF reflection height. Thus the VLF variations we observed here were most likely a result of the lower-energy ~100–300 keV electrons which might have accompanied the 2–6 MeV electrons, because these are the particles that produce most of the ionization enhancement in the *D* region where VLF waves are reflected. Unfortunately, the lower-energy (less than 2 MeV) channels on board SAMPEX are not reliable at all times, and thus these data were not suitable for this study.

[32] The PET instrument provides omnidirectional flux measurements of >0.4 MeV electrons. We used daily averaged measurements from the ELO channel which was designed to measure 2–6 MeV. The fluxes were mapped to nominal L shell distances using the International Geomagnetic Reference Field (IGRF) model. Using the daily averaged energetic (2–6 MeV) electron flux varying with L value from 2 to 7 [*Li et al.*, 2001], and our recorded VLF data from that period, we analyzed six nights, from day of year (DOY) 185 (3 July 2000) to DOY 210 (28 July 2000), of data from lightning occurring north (L value is from ~2.3 to 3.3) of Duke where energetic electron precipitation occurred. The probed regions in the six nights are shown in Figure 8. On these six nights, for the L shells we probed, the high-energy electron precipitation intensities were different, which suggests different ionosphere electron densities and, consequently, different nighttime ionosphere height parameter h' over these regions. We used the SAMPEX measured daily averaged flux at the path center's L value as the approximation of the corresponding daily average electron flux over each probed region, which revealed that on DOY 185, DOY 194, and DOY 196, the high-energy electron precipitation was low, that it was strong on DOY 201, and moderate on DOY 210 and DOY 219. This observation indicates that the ionospheric height parameter h' on DOY 201 might be expected to be the lowest as a result of the stronger electron precipitation, and that on DOY 185, DOY 194, and DOY 196, the height parameter h' should have been higher as a result of the weaker precipitation.

[33] By comparing the observed sferic spectra with the best fit modeled sferic spectra, we inferred the *D* region electron density profiles over the different probed regions, referred to sea level, as shown in Figure 9. Figure 10 shows the variations of the corresponding ionospheric height parameter h' with the estimated daily average energetic electron flux over the probed regions. Figure 10 indicates that there is an inverse correlation between energetic electron flux and the inferred h'. This inverse correlation is expected because the larger flux causes the stronger precipitations which decrease the ionospheric height parameter h'.

[34] This result suggests that the high-energy (2–6 MeV) electron precipitation, based on our measurements, appear to be accompanied by lower-energy ~100–300 keV electrons that are a significant source for night-to-night variations of the ionospheric *D* region electron density over the probed regions from 3 to 28 July 28 2000. The electron density profile variability of our measurements in July 2000 and the variability in July/August of 2004 are very similar; and, it is reasonable for us to attribute the variations of

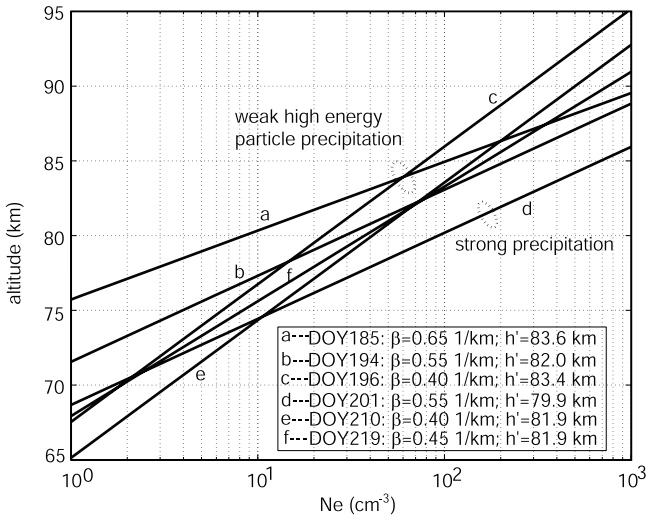

Figure 9. Best fit inferred *D* region electron density profiles from DOY 185 to DOY 210, 2000.

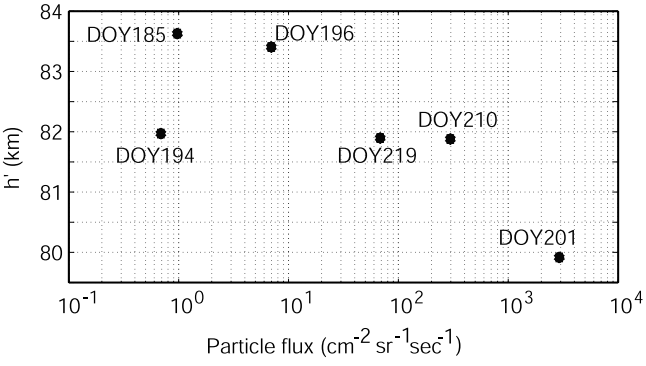

Figure 10. Inferred h' variation with the average energetic electron flux from DOY 185 to DOY 210, 2000.

nighttime ionospheric *D* region electron density in July/August of 2004 to the high-energy electron precipitation.

6. Summary and Conclusions

[35] Lightning-generated VLF energy is a useful tool for remotely sensing the nighttime ionospheric *D* region [*Cummer et al.*, 1998]. In an effort to better understand the nature of the nighttime ionospheric *D* region, we have applied this broadband VLF technique to infer the nighttime ionospheric *D* region electron densities over the United States east coast from 1 July to 4 August 2004.

[36] We used a two-dimensional, laterally homogenous LWPC model to model the theoretical propagation of the VLF radio atmospherics, in order to infer the electron density profile from measured VLF spectra. The sferic spectrum of the transverse horizontal magnetic field is a better indicator of the ionospheric parameters than its sferic waveform; thus all the comparisons of theory and observation were made in the frequency domain. The details of the sferic spectrum were shown to be strongly dependent on the height and sharpness of the two-parameter model ionosphere. Averaging and filtering techniques were used to improve the spectrum signal noise level.

[37] The measurement results of the 16 days from 1 July to 4 August 2004, show that the nighttime ionospheric *D* region is far from static. The ionospheric height parameter h' during that period was within the range of 82.0 ± 0.2 to 85.6 ± 0.2 km. However, for 13 out of 16 days, h' was within the range of 83.6 ± 0.2 to 85.6 ± 0.2 km, with the mean value equal to 84.5 ± 0.2 km, and, for only three out of 16 days, h' was below 83.0 ± 0.2 km. The ionospheric sharpness parameter β during that period was within the range of 0.40 ± 0.05 to 0.55 ± 0.05 km^{-1}. However, for 15 out of 16 days, β was within the range of 0.40 ± 0.05 to 0.50 ± 0.05 km^{-1}, with the mean value equal to 0.45 ± 0.05 km^{-1}, and, for only one day, β was greater than 0.50 ± 0.05 km^{-1}. The inferred profiles and variabilities of the nighttime ionospheric *D* region electron density from our measurements were in good agreement with those from past nighttime rocket experiments which had been made at similar latitudes. In addition, our measurement results in July 2000 exhibited a good correlation with the simultaneous SAMPEX precipitating electron measurement data.

[38] We conclude that night-to-night variations of the ionospheric *D* region electron densities can be reliably derived using broadband VLF energy radiated from lightning strokes. Our inferred electron density profile is the best exponential fit, in the electron density range of ~3 to ~500 cm^{-3}, to the rocket-measured electron density profile. High-energy electron precipitations might account for at least part of the night-to-night variations of the ionospheric *D* region electron densities at the midlatitudes.

[39] **Acknowledgments.** This research was supported by the NSF Aeronomy Program grant ATM-0092907. We thank M. Friedrich for sharing his archived rocket-measured *D* region electron density profiles and for useful discussions with him concerning the reliability of *D* region electron density.

[40] Arthur Richmond thanks J. Vincent Eccles and Craig J. Rodger for their assistance in evaluating this paper.

References

Bainbridge, G., and U. S. Inan (2003), Ionospheric *D* region electron density profiles derived from the measured interference pattern of VLF waveguide modes, *Radio Sci.*, *38*(4), 1077, doi:10.1029/2002RS002686.

Baker, D. N., R. A. Goldberg, F. A. Herrero, J. B. Blake, and L. B. Callis (1993a), Satellite and rocket studies of relativistic electrons and their influence on the middle atmosphere, *J. Atmos. Terr. Phys.*, *55*, 1619.

Baker, D. N., G. M. Mason, O. Figueroa, G. Colon, J. G. Watzin, and R. M. Aleman (1993b), An overview of the solar, anomalous, and magnetospheric particle explorer (SAMPEX) mission, *IEEE Trans. Geosci. Remote Sens.*, *31*(3), 531.

Bickel, J. E., J. A. Ferguson, and G. V. Stanley (1970), Experimental observation of magnetic field effects on VLF propagation at night, *Radio Sci.*, *5*, 19.

Brasseur, G., and J. B. Solomon (1984), *Aeronomy of the Middle Atmosphere*, Springer, New York.

Budden, K. G. (1961), *The Wave-Guide Mode Theory of the Wave Propagation*, Logos, London.

Budden, K. G. (1985), *The Propagation of Radio Waves*, Cambridge Univ. Press, New York.

Chilton, C. J. (1961), VLF phase perturbation associated with meteor shower ionization, *J. Geophys. Res.*, *66*, 379.

Cook, W. R., et al. (1993), PET: A proton/electron telescope for studies of magnetospheric, solar, and galactic particles, *IEEE Trans. Geosci. Remote Sens.*, *31*(3), 565.

Cummer, S. A., T. F. Bell, U. S. Inan, and D. L. Chenette (1997), VLF remote sensing of high-energy auroral particle precipitation, *J. Geophys. Res.*, *102*, 7477.

Cummer, S. A., U. S. Inan, and T. F. Bell (1998), Ionospheric *D* region remote sensing using VLF radio atmospherics, *Radio Sci.*, *33*, 1781.

Cummins, K. L., E. P. Krider, and M. D. Malone (1998), The US National Lightning Detection Network and applications of cloud-to-ground lightning data by electric power utilities, *IEEE Trans. Electromagn. Compat.*, *40*, 465–480.

Danilov, A. D., and L. B. Vanina (2001), Electron density variation in the polar *D* region from in situ measurements, *Int. J. Geomagn. Aeron.*, *2*(3), 195.

Deeks, D. G. (1966), *D*-region electron distributions in the middle latitudes deduced from the reflection of long radio waves, *Proc. R. Soc. London, Ser. A*, *291*, 413.

Dennis, A. S., and E. T. Pierce (1964), The return stroke of the lighting flash to Earth as a source of VLF atmospherics, *J. Res. Natl. Bur. Stand., Sect. D*, *68*, 777.

Fejer, J. A. (1970), Radio wave probing of the lower ionosphere by cross-modulation technique, *J. Atmos. Terr. Phys.*, *32*, 597.

Friedrich, M., and K. M. Torkar (2001), FIRI: A semiempirical model of the lower ionosphere, *J. Geophys. Res.*, *106*, 21,409.

Hargreaves, J. K. (1992), *The Solar-Terrestrial Environment*, Cambridge Univ. Press, New York.

Holt, O., and G. M. Lerfald (1967), Results from RF capacity probe experiment in the auroral ionosphere, *Radio Sci.*, *2*, 1283.

Inan, U. S., and A. S. Inan (1999), *Engineering Electromagnetics*, Addison-Wesley, Boston, Mass.

Inan, U. S., N. G. Lehtinen, S. J. Lev-Tov, M. P. Johnson, T. F. Bell, and K. Hurley (1999), Ionization of the lower ionosphere by γ-rays from a magnetar: Detection of a low energy (3–10 keV) component, *Geophys. Res. Lett.*, *26*(22), 3357.

Jacobsen, T. A., and M. Friedrich (1979), Electron density measurements in the lower *D* region, *J. Atmos. Terr. Phys.*, *41*, 1195.

Jones, D. L. (1970), Electromagnetic radiation from multiple return strokes of lightning, *J. Atmos. Terr. Phys.*, *32*, 1077.

Kikuchi, T., and D. S. Evans (1983), Quantitative study of substorm-associated VLF phase anomalies and precipitating energetic electrons on November 13, 1979, *J. Geophys. Res.*, *88*, 871.

Kopp, E., U. Jenzer, and K. Kazil (2003), Ions of the nighttime mid-latitude *E*- and *D*-regions: A comparison between measurements and the UBAIM ion model, in *16th ESA Symposium on European Rocket and Balloon Programmes and Related Research, 2–5 June 2003, Sankt Gallen, Switzerland*, edited by B. Warmbein, *Eur. Space Agency, Spec. Publ. ESA-SP 530*, 363.

Li, X., D. N. Baker, S. G. Kanekal, M. Looper, and M. Temerin (2001), Long term measurement of radiation belts by SAMPEX and their variations, *Geophys. Res. Lett.*, *28*, 3827.

Mathews, J. D., J. K. Breakall, and S. Ganguly (1982), The measurement of diurnal variations of electron concentration in the 60–100 km ionosphere at Arecibo, *J. Atmos. Terr. Phys.*, *44*, 441.

Mechtly, E. A., and L. G. Smith (1968), Growth of the *D*-region at sunrise, *J. Atmos. Terr. Phys.*, *30*, 363.

Mechtly, E. A., S. A. Bowhill, L. G. Smith, and H. W. Knoebel (1967), Lower ionosphere electron concentration and collision frequency from

rocket measurements of Faraday rotation, differential absorption, and probe current, *J. Geophys. Res.*, *72*, 5239.

Morfitt, D. G., and C. H. Shellman (1976), MODESRCH: An improved computer program for obtaining ELF/VLF/LF mode constants in an Earth-ionosphere waveguide, *Interim Rep. 77T*, Nav. Electron. Lab. Cent., San Diego, Calif.

Narcisi, R. S. (1971), Composition studies of the lower ionosphere, in *Physics of the Upper Atmosphere*, edited by F. Verniani, Ed. Compositori, Bologna, Italy. (Reprinted in *Handbook of Geophysics and the Space Environment*, edited by Adolph S. Jursa, pp. 21–56, Air Force Geophys. Lab, Air Force Syst. Command, Springfield, Va., 1985.)

Narcisi, R. S., and A. D. Bailey (1965), Mass spectrometric measurements of positive ions at altitudes from 64–112 kilometers, *J. Geophys. Res.*, *70*, 3687.

Newman, D. B., and A. J. Ferraro (1976), Amplitude distributions of partially reflected signals from the mid-latitude *D*-region, *J. Geophys. Res.*, *81*, 2442.

Pappert, R. A., and J. A. Ferguson (1986), VLF/LF mode conversion model calculations for air to air transmissions in the Earth-ionosphere waveguide, *Radio Sci.*, *21*, 551.

Rees, M. H. (1989), *Physics and Chemistry of the Upper Atmosphere*, Cambridge Univ. Press, New York.

Sechrist, C. F., Jr. (1974), Comparisons of techniques for measurement of *D* region electron densities, *Radio Sci.*, *9*, 137.

Seddon, J. C. (1953), Propagation measurements in the ionosphere with the aid of rockets, *J. Geophys. Res.*, *58*, 323.

Smith, L. G. (1969), *Langmuir Probes in the Ionosphere*, 261 pp., Elsevier, New York.

Smith, L. G., and B. E. Gilchrist (1984), Rocket observations of electron density in the nighttime *E*-region using Faraday rotation, *Radio Sci.*, *19*, 913.

Thomas, L., and M. D. Harrison (1970), The electron density distribution in the *D*-region during the night and pre-sunrise period, *J. Atmos. Terr. Phys.*, *32*, 1.

Thomson, N. R. (1993), Experimental daytime VLF ionospheric parameters, *J. Atmos. Terr. Phys.*, *55*, 173.

Thomson, N. R., C. J. Rodger, and M. A. Clilverd (2005), Large solar flares and their ionospheric *D* region enhancements, *J. Geophys. Res.*, *110*, A06306, doi:10.1029/2005JA011008.

Uman, M. (1987), *Lightning Discharge*, Elsevier, New York.

Wait, J. R., and K. P. Spies (1964), Characteristics of the Earth-ionosphere waveguide for VLF radio waves, *Tech. Note 300*, Natl. Bur. of Stand., Boulder, Colo.

D. N. Baker, Laboratory for Atmospheric and Space Physics, University of Colorado, Boulder, CO 80309, USA. (daniel.baker@lasp.colorado.edu)

Z. Cheng and S. A. Cummer, Department of Electrical and Computer Engineering, Duke University, Durham, NC 27708, USA. (zc@ee.duke.edu; cummer@ee.duke.edu)

S. G. Kanekal, SEC, NOAA, 325 Broadway, Boulder, CO 80305, USA. (shrikanth.kanekal@noaa.gov)